



HAL
open science

Numerical modelling of the healing process induced by carbonation of a single crack in concrete structures: Theoretical formulation and Embedded Finite Element Method implementation

Harifidy Ranaivomanana, Nathan Benkemoun

► **To cite this version:**

Harifidy Ranaivomanana, Nathan Benkemoun. Numerical modelling of the healing process induced by carbonation of a single crack in concrete structures: Theoretical formulation and Embedded Finite Element Method implementation. *Finite Elements in Analysis and Design*, 2017, 132, pp.42-51. 10.1016/J.finel.2017.05.003 . hal-04194704

HAL Id: hal-04194704

<https://hal.science/hal-04194704>

Submitted on 17 Nov 2023

HAL is a multi-disciplinary open access archive for the deposit and dissemination of scientific research documents, whether they are published or not. The documents may come from teaching and research institutions in France or abroad, or from public or private research centers.

L'archive ouverte pluridisciplinaire **HAL**, est destinée au dépôt et à la diffusion de documents scientifiques de niveau recherche, publiés ou non, émanant des établissements d'enseignement et de recherche français ou étrangers, des laboratoires publics ou privés.

Numerical modelling of the healing process induced by carbonation of a single crack in concrete structures : Theoretical formulation and Embedded Finite Element Method implementation

Ranaivomanana, H.^a, Benkemoun N.^{a,*}

^a *Université Nantes Angers Le Mans (L'UNAM), GeM,
Research Institute of Civil Engineering and Mechanics, CNRS UMR 6183, Nantes University, IUT
Saint-Nazaire
58 rue Michel Ange, 44600 Saint-Nazaire, FRANCE*

Abstract

We consider a model for reactive flows which describes the healing process induced by carbonation of a single crack in concrete structures. The aim of this paper is to study the complex interplay between advection-diffusion mechanisms in a crack-matrix system combined with different chemical reactions taking place (dissolution/precipitation). Carbonated water is first injected through a crack. Then, a diffusion process of calcium ions (C_a^{2+}) takes place from the porous matrix to the crack due to the existing calcium ions concentration gradient. Finally, those calcium and carbonates ions (CO_3^{2-}) from the percolating solution react to form a calcite (C_aCO_3) layer responsible for the healing of the crack. The developed model takes the form of transport-reaction partial differential equations for both crack and porous matrix. From numerical point of view these equations are discretized by means of the Embedded Finite Element Method (E-FEM). The E-FEM allows to use meshes not necessarily matching the physical interface, defined herein as the crack, while retaining the accuracy of the classical finite element approach. This is achieved by introducing a weak discontinuity in the calcium ions concentration field for finite elements where the crack is present. A numerical solving strategy is presented to efficiently resolve the FE problem both in terms of calcium and carbonate concentration field variables and weak discontinuity parameters. In addition, an analytical model for the computation of the calcite layer width, resulting in the healing process, is suggested. Finally, considering the dependence of the

diffusivity and permeability coefficients on the width of the calcite, a coupled model arises for the numerical modelling of the healing process induced by carbonation in a crack.

Keywords: Embedded Finite Element formulation; EAS method; Weak Discontinuity; Healing process; Concrete; Crack; Structure durability;

1. Introduction

The assessment of concrete structure lifetime is nowadays necessary for the design of durable structures. As a complementary means to experimental approaches, numerical modelling can be a relevant tool for this lifetime assessment. The development of thorough numerical models requires a comprehension not only of the degradation phenomena but also of the healing process. Indeed, healing process can improve the durability of structures (storage or containment structures for instance). The healing process can occur in both ways (see [1], [2] and [3]):

- *naturally* by calcium carbonate formation, expansion of hydrated cementitious matrix, blocking of cracks by impurities present in water (sealing) and further hydration of unreacted cement.
- *artificially* by the use of chemical admixtures, polymers and geo-materials and even microorganism which are able to produce calcium carbonates.

Among the natural healing processes mentionned above, the formation of calcium carbonate is investigated in this study, since it is considered as one of the most promising autogenous healing mechanisms (see [4], [5], [6] or [7] for a review and [8] for experimental results concerning microbially-induced calcium carbonate precipitation). Most publications dedicated to the modeling of natural self-healing process mainly concern the process of further hydration of unreacted cement ([1], [9], [10] and [11]). However concerning the modeling of the natural self-healing process induced by carbonation, there is not so much information in

*Corresponding author.

Email address: `nathan.benkemoun@univ-nantes.fr` (Benkemoun N.)

21 the literature. The authors in [6] have proposed a simplified model for the evolution of the
22 leakage rate through a cracked material versus time, while carbonated water flows through
23 the crack. However, their approach is limited by the fact that two calibration parameters,
24 whose values vary from one material to another, are present in the model. In [12], the authors
25 have developed a multiple phase self-healing-model, that simulates three distinct stages in
26 the healing process: fracture process, transport of healing agents to the healing location
27 and mechanical strength recovery. The authors introduced a hygro-chemical transportation
28 model (momentum and mass balance equations), in which the active species are transported
29 by advective, diffusive and dispersive fluxes through the pore fluid to damaging and heal-
30 ing sites. More recently, [13] have proposed a finite-element model describing self-healing
31 mechanisms in engineered cementitious composites and based on C_aCO_3 precipitation. The
32 model takes into account the diffusive mechanisms of aqueous species in the material, and
33 the most fundamental chemical equations that take place during the healing phenomenon.
34 The concentration of the three main species (calcium ions C_a^{2+} , carbonate ions CO_3^{2-} and
35 calcite C_aCO_3) acting on the healing process are identified as the main model variables and
36 the modeling results into a reaction-diffusive set of equations. However, the model requires
37 further validations. Indeed simplified assumptions are assumed by the authors such as the
38 fact that the diffusion coefficients are independent from damage and healing variables. In
39 addition no water-flowing through the crack is considered.

40 In this paper, a numerical approach is presented in the context of the natural healing
41 process. In this sense, we suggest a numerical model for the healing process induced by
42 carbonation of a single crack in concrete structures. Transport equations of C_a^{2+} and CO_3^{2-}
43 written in the crack and transport equation of C_a^{2+} written in the porous media are consid-
44 ered and discretized by means of the Embedded Finite Element Method (E-FEM, see [14]
45 for instance). The E-FEM allows to use meshes not necessarily matching the physical inter-
46 face, defined herein as the crack, while retaining the accuracy of the classical finite element
47 approach. This is achieved by considering a weak discontinuity [15] in the calcium ions con-
48 centration field for finite elements where the crack is present. This enhancement, introduced
49 in the framework of the EAS method [16], allows to have the calcium ions concentration

50 field continuous itself and a jump in the normal direction of the calcium ions concentration
51 gradient, when passing through the crack. This results in a discontinuous leakage flux that
52 flows from the porous matrix toward the crack. This flux represents the mass coupling term
53 between the porous media surrounding the crack and the crack itself. It is important to
54 stress the fact that this coupling term arises naturally in the weak form of the problem,
55 since the crack is directly embedded in the mesh through the E-FEM. This a serious ad-
56 vantage when the FE discretization is performed. Finally, having at hands the calcite and
57 calcium concentration fields values for each time step, the width of the calcite layer in the
58 crack is computed by means of an analytical model, resulting in the healing process in the
59 crack. Finally, considering the fact that diffusivity and permeability coefficients values also
60 depend on this calcite layer width, a coupled model arises for the numerical modelling of
61 the healing process induced by carbonation in a crack.

62 The outline of this paper is as follows. In Section 2, the governing equations of the
63 problem are introduced. They consist in the transport equation of C_a^{2+} in the porous media
64 and in the crack, and the transport equation of CO_3^{2-} in the crack. In Section 3, the weak
65 form of the problem is suggested. It is obtained by means of the Galerkin approximation,
66 leading to the FE to be solved. In Section 4, the method to compute the coupling term
67 is shown. Also we present the analytical model to evaluate the width of the calcite layer,
68 resulting in the healing process. In Section 5, the FE discretization of the concentration
69 fields, based upon the E-FEM, and the solving strategy are presented.

70 **2. Governing equations**

71 In this section a model for reactive flows which describes the healing process induced by
72 carbonation of a single crack in concrete structures is considered. In this sense, the strong
73 form of the model governing equations is presented. We consider the transport equations
74 of C_a^{2+} and CO_3^{2-} written in the crack and the transport equation of C_a^{2+} written in the
75 porous media. Also chemical reactions (dissolution/precipitation) in the porous matrix and
76 the crack are regarded.

77 Technically speaking, carbonated water is first injected through the crack. Then, a
 78 diffusion process of calcium ions (C_a^{2+}) takes place from the porous matrix to the crack due
 79 to the existing calcium ions concentration gradient. Finally, those calcium and carbonates
 80 ions (CO_3^{2-}) from the percolating solution react to form a calcite (C_aCO_3) layer responsible
 81 for the healing of the crack. Those mechanisms are illustrated in Fig. 1 and are described
 82 hereafter for each transport equation.

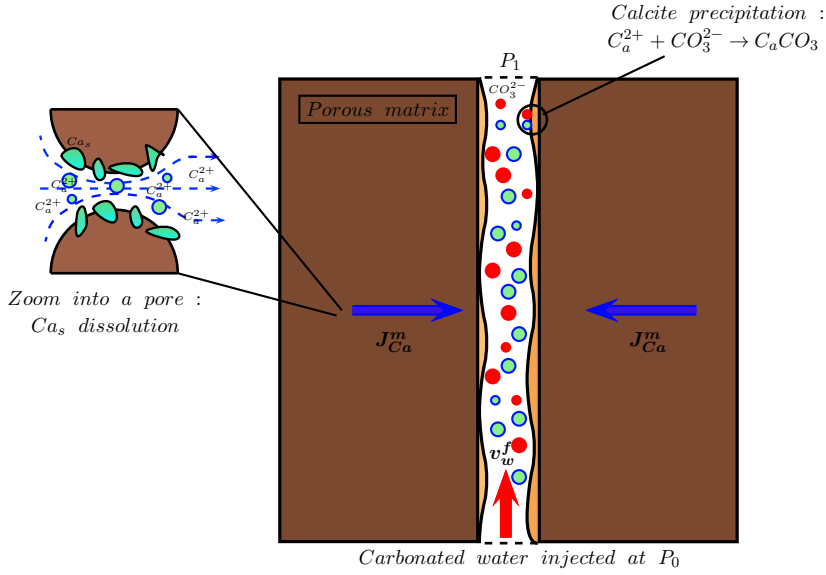


Figure 1: Schematic of the mechanisms taking place during the healing process induced by carbonation into a single crack

83 2.1. Transport equation of C_a^{2+} in the porous media

84 We note C_{Ca} the calcium ions concentration in the pore solution of the matrix, Φ^m the
 85 matrix porosity and φ_{Ca_s} a source term taking into account the dissolution of the calcium
 86 in the solid phase Ca_s . Transport by diffusion, resulting from the existing calcium ions
 87 concentration gradient between the crack and the porous matrix, is considered through the
 88 flux \mathbf{J}_{Ca}^m . Consequently, the transport equation (diffusion equation) of C_a^{2+} in the porous
 89 media is such as:

$$\frac{\partial \Phi^m C_{Ca}}{\partial t} + \nabla \cdot (\mathbf{J}_{Ca}^m) = \Phi^m \varphi_{Ca_s} \quad (1)$$

90 *2.2. Transport equation of C_a^{2+} in the crack*

91 Transport by diffusion and permeation is considered through the fluxes \mathbf{J}_{Ca}^f and $\Phi^f C_{Ca} \mathbf{v}_w^f$,
 92 respectively. Again transport by diffusion, resulting from the existing calcium ions concen-
 93 tration gradient between the crack and the porous matrix, is considered through the flux
 94 \mathbf{J}_{Ca}^m . Transport by permeation takes place because of the pressure gradient in between the
 95 bottom and the top side of the crack (see Fig. 1: $\nabla p_w = P_1 - P_0$). We note \mathbf{v}_w^f the fluid
 96 velocity and Φ^f the crack porosity. Last but not least, considering the fact that the C_a^{2+}
 97 and CO_3^{2-} ions react together all over the time to form calcite C_aCO_3 into the crack, the
 98 evolution of calcite formation has to be also taken into account. This is achieved by means
 99 of the source term $-\frac{\partial \xi}{\partial t}$ where ξ is the amount of calcite formed in the crack. This formation
 100 of calcite results in the healing process taking place into the crack.

101 This leads to the following transport equation (diffusion-permeation equation) of C_a^{2+} in
 102 the crack:

$$\frac{\partial \Phi^f C_{Ca}}{\partial t} + \nabla \cdot (\mathbf{J}_{Ca}^f) + \nabla \cdot (\Phi^f C_{Ca} \mathbf{v}_w^f) = -\frac{\partial \xi}{\partial t} \quad (2)$$

103 *2.3. Transport equation of CO_3^{2-} in the crack*

104 We note C_{CO_3} the carbonate ions concentration in the crack. Transport by permeation is
 105 considered through the flux $\Phi^f C_{CO_3} \mathbf{v}_w^f$. It takes place also because of the pressure gradient
 106 in between the bottom and the top side of the crack.

107 The transport equation of CO_3^{2-} in the crack is such as:

$$\frac{\partial \Phi^f C_{CO_3}}{\partial t} + \nabla \cdot (\Phi^f C_{CO_3} \mathbf{v}_w^f) = -\frac{\partial \xi}{\partial t} \quad (3)$$

108 The amount of C_aCO_3 , labeled as ξ , created in the crack is evaluated by means of the
 109 following relation:

$$\frac{\partial \xi}{\partial t} = K C_{Ca} C_{CO_3} \quad (4)$$

110 with K a constant value.

111 Last but not least, it is important to stress the fact that the diffusion model suggested
 112 in this paper based on Fick's Law oversimplifies some physical phenomena. For instance,
 113 the electrical coupling between the ions and its effect on their movements is overlooked. It
 114 is worth noting because it can influence the kinetic of calcite formation and consequently
 115 the healing process.

116 Having at hands the strong form of the transport equations, we now turn to Galerkin
 117 approximation of these equations.

118 3. Galerkin approximation: weak form of the transport equations

The domain Ω considered for the problem is shown in 2D in Fig. 2. We note $\partial\Omega$ the external boundary where essential and natural boundary conditions are prescribed. Also this domain contains a geometrical discontinuity labeled as Γ_d . We note Γ_d^+ and Γ_d^- the boundary of the discontinuity domain. The essential boundary conditions are imposed on $\partial\Omega$ such as

$$C_{Ca} = \bar{C}_{Ca} \text{ on } \partial\Omega_{Ca}, \quad (5)$$

119 where \bar{C}_{Ca} is the imposed calcium ions concentration on $\partial\Omega_{Ca}$.

The natural boundary conditions are imposed on $\partial\Omega$ such as

$$\mathbf{J}_{Ca}^m \cdot \mathbf{n} = \bar{J}_{Ca}^m \text{ on } \partial\Omega_{J_{Ca}^m}. \quad (6)$$

120 We note \bar{J}_{Ca}^m the prescribed flux over $\partial\Omega_{J_{Ca}^m}$ and \mathbf{n} the unit outward normal vector to the
 121 external boundary $\partial\Omega$, where the usual condition $\partial\Omega_{Ca} \cup \partial\Omega_{J_{Ca}^m} = \partial\Omega$ has to be respected.

In addition, considering the fact that there is a geometrical discontinuity Γ_d embedded in the domain Ω , a mass transfer coupling between the porous bulk material surrounding the crack and the crack itself arises. In this paper, this mass transfer comes from the exchange by diffusion of the calcium ions flow between the porous matrix surrounding the crack and the crack itself. Consequently, on Γ_d we have:

$$[[\mathbf{J}_{Ca}^m]] \cdot \mathbf{n}_{\Gamma_d} = J_{\Gamma_d} \text{ on } \Gamma_d \quad (7)$$

122 We note J_{Γ_d} the leakage flux of calcium ions induced by diffusion from the porous matrix
 123 toward the crack. As stated in [17] and [18] in the context of the X-FEM and in [19] in
 124 the context of the E-FEM, the normal component of this leakage flux is discontinuous when
 125 passing across Γ_d . The physical meaning of this discontinuity is that a part of the calcium
 126 ions flow induced by diffusion that enters in the crack through one of its faces flows away
 127 tangentially when inside the crack or can even be stored within the crack. Consequently
 128 the flux of calcium ions normal to the crack is discontinuous. We refer \mathbf{n}_{Γ_d} as the the unit
 129 normal vector to the discontinuity Γ_d pointing out to Ω^+ and $[\![\bullet]\!] = \bullet^+ - \bullet^-$ as the jump
 130 between the values at Γ_d^+ and Γ_d^- sides.

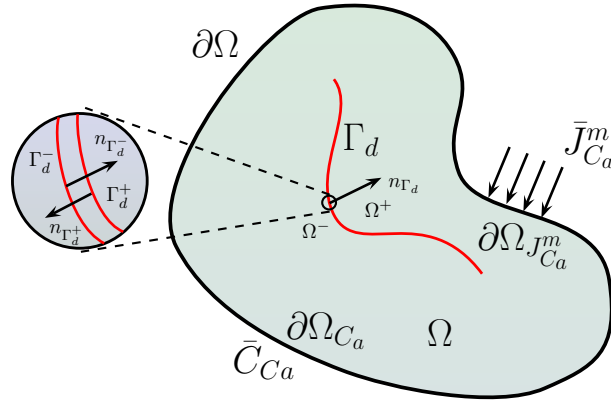


Figure 2: Illustration of the domain Ω including the discontinuity Γ_d and the boundary conditions (inspired from [17])

131 3.1. Weak form of 1

132 The discrete form of eqn. 1 is obtained by employing the Galerkin approximation. This
 133 approximation leads to :

$$\int_{\Omega} \delta C_{Ca} \frac{\partial \Phi^m C_{Ca}}{\partial t} d\Omega + \int_{\Omega} \delta C_{Ca} \nabla \cdot (\mathbf{J}_{Ca}^m) d\Omega = \int_{\Omega} \delta C_{Ca} \Phi^m \varphi_{Ca_s} d\Omega, \quad (8)$$

134 where δC_{Ca} is the virtual ions calcium concentration in the space \mathcal{C} such as $\mathcal{C} = \{\delta C_{Ca} :$
 135 $\Omega \mapsto \mathbb{R} \mid \delta C_{Ca} \in H^1, \delta C_{Ca} = 0 \text{ on } \partial\Omega_{C_a}\}$.

Using the divergence theorem on the second term of eqn. 8 left hand side yields:

$$\begin{aligned} \int_{\Omega} \delta C_{Ca} \nabla \cdot (\mathbf{J}_{Ca}^m) d\Omega &= - \int_{\Omega} \nabla(\delta C_{Ca}) \cdot \mathbf{J}_{Ca}^m d\Omega + \int_{\partial\Omega_{J_{Ca}^m}} \delta C_{Ca} \bar{J}_{Ca}^m d\partial\Omega + \int_{\Gamma_d^+} \delta C_{Ca}^+ (\mathbf{J}_{Ca}^{m,+} \cdot \mathbf{n}_{\Gamma_d^+}) d\Gamma \\ &+ \int_{\Gamma_d^-} \delta C_{Ca}^- (\mathbf{J}_{Ca}^{m,-} \cdot \mathbf{n}_{\Gamma_d^-}) d\Gamma, \end{aligned} \quad (9)$$

136 where eqn. 6 on $\partial\Omega_{J_{Ca}^m}$ and $\delta C_{Ca} = 0$ on $\partial\Omega_{Ca}$ have been considered.

Assuming the fact that the calcium ions concentration has the same value at both faces of the crack ([18] and [17]): $C_{Ca}^+ = C_{Ca}^- = C_{Ca}$ and considering a Bubnov-Galerkin approach, the virtual calcium ions concentration at both faces is such as $\delta C_{Ca}^+ = \delta C_{Ca}^- = \delta C_{Ca}$. Finally invoking $\mathbf{n}_{\Gamma_d^-} = -\mathbf{n}_{\Gamma_d^+} = \mathbf{n}_{\Gamma_d}$, we obtain

$$\int_{\Omega} \delta C_{Ca} \nabla \cdot (\mathbf{J}_{Ca}^m) d\Omega = - \int_{\Omega} \nabla(\delta C_{Ca}) \cdot \mathbf{J}_{Ca}^m d\Omega + \int_{\partial\Omega_{J_{Ca}^m}} \delta C_{Ca} \bar{J}_{Ca}^m d\partial\Omega - \int_{\Gamma_d} \delta C_{Ca} J_{\Gamma_d} d\Gamma, \quad (10)$$

137 where eqn. 7 has been considered on Γ_d .

138 Note that considering the same value for the calcium ions concentrations at both faces of
139 the crack and in a more general manner considering an “hydraulic” variable as continuous
140 passing through a crack is not something agreed in the computational mechanics commu-
141 nity. An enlightening classification can be found in [20] where the author describes both
142 continuous and discontinuous approaches for modelling the pressure field passing across a
143 crack. The author shows that the discontinuity in the pressure field can be taken into ac-
144 count by considering (1) a jump in the pressure field or (2) a jump in the pressure field
145 plus an independent pressure at the discontinuity. The choice between (1) and (2) being
146 done regarding the physics of the problem. In [19], a discontinuous capillary pressure is also
147 considered accross a crack. In this case it is to fit the required nodal conditions imposed
148 by the G-FEM for the capillary pressure field discretization.

149 Finally combining eqn. 10 and 8, we obtain

$$\begin{aligned} &\int_{\Omega} \delta C_{Ca} \frac{\partial \Phi^m C_{Ca}}{\partial t} d\Omega - \int_{\Omega} \nabla(\delta C_{Ca}) \cdot \mathbf{J}_{Ca}^m d\Omega + \int_{\partial\Omega_{J_{Ca}^m}} \delta C_{Ca} \bar{J}_{Ca}^m d\partial\Omega - \int_{\Gamma_d} \delta C_{Ca} J_{\Gamma_d} d\Gamma \\ &= \int_{\Omega} \delta C_{Ca} \Phi^m \varphi_{Ca_s} d\Omega, \end{aligned} \quad (11)$$

150 The sign - before the coupling term $\int_{\Gamma_d} \delta C_{Ca} J_{\Gamma_d} d\Gamma$ indicates that J_{Γ_d} “leaves” the bulk
 151 material surrounding the crack and flows toward the crack. It is important to note that
 152 the coupling term, representing the exchange by diffusion of the calcium ions flow between
 153 the porous matrix surrounding the crack and the crack itself, arises naturally in the weak
 154 form of the transport equation (eqn. 1) since the discontinuity (crack) is embedded into the
 155 problem.

156 3.2. Weak form of 2

157 The discrete form of eqn. 9 is obtained by employing the Galerkin approximation. This
 158 approximation leads to :

$$\begin{aligned} & \int_{\Omega_d} \delta C_{Ca} \frac{\partial \Phi^f C_{Ca}}{\partial t} d\Omega + \int_{\Omega_d} \delta C_{Ca} \nabla \cdot (\mathbf{J}_{Ca}^f) d\Omega + \int_{\Omega_d} \delta C_{Ca} \nabla \cdot (\Phi^f C_{Ca} \mathbf{v}_w^f) d\Omega \\ & = - \int_{\Omega_d} \delta C_{Ca} \frac{\partial \xi}{\partial t} d\Omega, \end{aligned} \quad (12)$$

159 where δC_{Ca} is the virtual ions calcium concentration in the space $\mathcal{C}_{d,Ca}$ such as $\mathcal{C}_{d,Ca} = \{\delta C_{Ca} :$
 160 $\Omega_d \mapsto \mathbb{R} \mid \delta C_{Ca} \in H^1, \delta C_{Ca} = 0 \text{ on } \partial\Omega_{d,Ca}\}$. We note Ω_d the domain of the discontinuity.

Using now the divergence theorem on the second term of eqn. 12 yields:

$$\begin{aligned} \int_{\Omega_d} \delta C_{Ca} \nabla \cdot (\mathbf{J}_{Ca}^f) d\Omega & = - \int_{\Omega_d} \nabla(\delta C_{Ca}) \cdot (\mathbf{J}_{Ca}^f) d\Omega + \int_{\Gamma_d^+} \delta C_{Ca}^+ (\mathbf{J}_{Ca}^{f,+} \cdot \mathbf{n}_{\Gamma_d^+}) d\Gamma \\ & + \int_{\Gamma_d^-} \delta C_{Ca}^- (\mathbf{J}_{Ca}^{f,-} \cdot \mathbf{n}_{\Gamma_d^-}) d\Gamma \end{aligned} \quad (13)$$

Considering the fact that the calcium ions flow between the porous matrix surrounding
 the crack and the crack itself is continuous at each of the faces Γ_d^+ and Γ_d^- of the discontinuity
 domain (see [18] for the same argument) :

$$\mathbf{J}_{Ca}^{f,+} = \mathbf{J}_{Ca}^{m,+} \quad \text{and} \quad \mathbf{J}_{Ca}^{f,-} = \mathbf{J}_{Ca}^{m,-}, \quad (14)$$

161 the convention for the unit normal vectors within the discontinuity domain Ω_d : $-\mathbf{n}_{\Gamma_d^-} =$
 162 $\mathbf{n}_{\Gamma_d^+} = \mathbf{n}_{\Gamma_d}$ (opposite to the convention for unit normal vectors within the domain Ω) and
 163 $\delta C_{Ca}^+ = \delta C_{Ca}^- = \delta C_{Ca}$ lead to

$$\int_{\Omega_d} \delta C_{Ca} \nabla \cdot (\mathbf{J}_{Ca}^f) d\Omega = - \int_{\Omega_d} \nabla(\delta C_{Ca}) \cdot (\mathbf{J}_{Ca}^f) d\Omega + \int_{\Gamma_d} \delta C_{Ca} J_{\Gamma_d} d\Gamma \quad (15)$$

164 where eqn. 7 has been considered on Γ_d .

Using the divergence theorem on the third term of eqn. 12 yields:

$$\begin{aligned} \int_{\Omega_d} \delta C_{Ca} \nabla \cdot (\Phi^f C_{Ca} \mathbf{v}_w^f) d\Omega &= - \int_{\Omega_d} \nabla(\delta C_{Ca}) \cdot (\Phi^f C_{Ca} \mathbf{v}_w^f) d\Omega + \int_{\Gamma_d^+} \delta C_{Ca}^+ (\Phi^f C_{Ca}^+ \mathbf{v}_w^{f,+}) \cdot \mathbf{n}_{\Gamma_d^+} d\Gamma \\ &+ \int_{\Gamma_d^-} \delta C_{Ca}^- (\Phi^f C_{Ca}^- \mathbf{v}_w^{f,-}) \cdot \mathbf{n}_{\Gamma_d^-} d\Gamma \end{aligned} \quad (16)$$

Invoking the arguments : $C_{Ca}^+ = C_{Ca}^- = C_{Ca}$, $\delta C_{Ca}^+ = \delta C_{Ca}^- = \delta C_{Ca}$, $-\mathbf{n}_{\Gamma_d^-} = \mathbf{n}_{\Gamma_d^+} = \mathbf{n}_{\Gamma_d}$ and $\mathbf{v}_w^{f,-} = \mathbf{v}_w^{f,+} = \mathbf{v}_w^f$ in the domain Ω_d leads to

$$\int_{\Omega_d} \delta C_{Ca} \nabla \cdot (\Phi^f C_{Ca} \mathbf{v}_w^f) d\Omega = - \int_{\Omega_d} \nabla(\delta C_{Ca}) \cdot (\Phi^f C_{Ca} \mathbf{v}_w^f) d\Omega \quad (17)$$

Finally combining eqn. 15, eqn. 17 and 12 gives:

$$\begin{aligned} \int_{\Omega_d} \delta C_{Ca} \frac{\partial \Phi^f C_{Ca}}{\partial t} d\Omega - \int_{\Omega_d} \nabla(\delta C_{Ca}) \cdot (\Phi^f C_{Ca} \mathbf{v}_w^f) d\Omega - \int_{\Omega_d} \nabla(\delta C_{Ca}) \cdot (\mathbf{J}_{Ca}^f) d\Omega + \int_{\Gamma_d} \delta C_{Ca} J_{\Gamma_d} d\Gamma \\ = - \int_{\Omega_d} \delta C_{Ca} \frac{\partial \xi}{\partial t} d\Omega \end{aligned} \quad (18)$$

165 The sign + before the term $\int_{\Gamma_d} \delta C_{Ca} J_{\Gamma_d} d\Gamma$ indicates that J_{Γ_d} flows towards the crack
166 and “leaves” the bulk material surrounding the crack. Again the coupling term appears
167 naturally in the weak form (eqn. 18).

168 3.3. Weak form of \mathcal{B}

169 The discrete form of eqn. 10 is obtained by employing the Galerkin approximation. This
170 approximation leads to :

$$\int_{\Omega_d} \delta C_{CO_3} \frac{\partial \Phi^f C_{CO_3}}{\partial t} d\Omega + \int_{\Omega_d} \delta C_{CO_3} \nabla \cdot (\Phi^f C_{CO_3} \mathbf{v}_w^f) d\Omega = - \int_{\Omega_d} \delta C_{CO_3} \frac{\partial \xi}{\partial t} d\Omega \quad (19)$$

171 where δC_{CO_3} is the virtual ions carbonate concentration in the space \mathcal{C}_{d,CO_3} such as \mathcal{C}_{d,CO_3}
172 = $\{\delta C_{CO_3} : \Omega_d \mapsto \mathbb{R} \mid \delta C_{CO_3} \in H^1, \delta C_{CO_3} = 0 \text{ on } \partial\Omega_{d,CO_3}\}$.

Using now the divergence theorem on the second term of eqn. 19 yields:

$$\begin{aligned} \int_{\Omega_d} \delta C_{CO_3} \nabla \cdot (\Phi^f C_{CO_3} \mathbf{v}_w^f) d\Omega &= - \int_{\Omega_d} \nabla(\delta C_{CO_3}) \cdot (\Phi^f C_{CO_3} \mathbf{v}_w^f) d\Omega + \int_{\Gamma_d^+} \delta C_{CO_3}^+ (\Phi^f C_{CO_3}^+ \mathbf{v}_w^{f,+}) \cdot \mathbf{n}_{\Gamma_d^+} d\Gamma \\ &+ \int_{\Gamma_d^-} \delta C_{CO_3}^- (\Phi^f C_{CO_3}^- \mathbf{v}_w^{f,-}) \cdot \mathbf{n}_{\Gamma_d^-} d\Gamma \end{aligned} \quad (20)$$

173 Invoking the arguments: $C_{CO_3}^+ = C_{CO_3}^- = C_{CO_3}$, $\delta C_{CO_3}^+ = \delta C_{CO_3}^- = \delta C_{CO_3}$ (Bubnov-
174 Galerkin approach also considered for δC_{CO_3}), $-\mathbf{n}_{\Gamma_d^-} = \mathbf{n}_{\Gamma_d^+} = \mathbf{n}_{\Gamma_d}$ and $\mathbf{v}_w^{f,-} = \mathbf{v}_w^{f,+} = \mathbf{v}_w^f$
175 in the domain Ω_d leads to

$$\int_{\Omega_d} \delta C_{CO_3} \nabla \cdot (\Phi^f C_{CO_3} \mathbf{v}_w^f) d\Omega = - \int_{\Omega_d} \nabla(\delta C_{CO_3}) \cdot (\Phi^f C_{CO_3} \mathbf{v}_w^f) d\Omega \quad (21)$$

Finally combining eqn. 21 and eqn. 19 gives

$$\int_{\Omega_d} \delta C_{CO_3} \frac{\partial \Phi^f C_{CO_3}}{\partial t} d\Omega - \int_{\Omega_d} \nabla(\delta C_{CO_3}) \cdot (\Phi^f C_{CO_3} \mathbf{v}_w^f) d\Omega = - \int_{\Omega_d} \delta C_{CO_3} \frac{\partial \xi}{\partial t} d\Omega \quad (22)$$

176 4. Evaluation of the coupling term $\int_{\Gamma_d} \delta C_{Ca} J_{\Gamma_d} d\Gamma$

177 4.1. Numerical hypothesis within the crack

In order to evaluate the coupling term $\int_{\Gamma_d} \delta C_{Ca} J_{\Gamma_d} d\Gamma$ present in eqn. 11, we use eqn. 18 to express it as a function of the integrals on Ω_d :

$$\begin{aligned} \int_{\Gamma_d} \delta C_{Ca} J_{\Gamma_d} d\Gamma &= - \int_{\Omega_d} \delta C_{Ca} \frac{\partial \Phi^f C_{Ca}}{\partial t} d\Omega + \int_{\Omega_d} \nabla(\delta C_{Ca}) \cdot (\Phi^f C_{Ca} \mathbf{v}_w^f) d\Omega \\ &+ \int_{\Omega_d} \nabla(\delta C_{Ca}) \cdot (\mathbf{J}_{Ca}^f) d\Omega - \int_{\Omega_d} \delta C_{Ca} \frac{\partial \xi}{\partial t} d\Omega \end{aligned} \quad (23)$$

178 This approach is also retained in [17] for an hydraulic crack problem. Nevertheless
179 terms related to the mechanical problem are furthermore present in this case. In [18], the
180 author proposes two ways to handle the coupling. The first way is very close to the one
181 presented in this paper and in [17]. The second way considers the crack totally filled by the
182 fluid (no deformable solid in the crack). Starting from the fluid mass conservation equation
183 in the crack, the author obtains the expression of the mass coupling term that resembles
184 to Reynolds lubrication equation (see [20]). This approach is also present in [21].

185 Hereafter the coupling term is evaluated in the local cartesian coordinate system (x_d, y_d) .
 186 x_d and y_d are in the directions of the normal and tangent unit vectors to the discontinuity,
 187 \mathbf{n}_{Γ_d} and \mathbf{t}_{Γ_d} . We assume that:

- 188 • the width of the crack $2h$ is negligible compared to its length (see [17] and [18] for the
 189 same argument). Consequently the variation of the calcium ions concentration in the
 190 \mathbf{n}_{Γ_d} direction is not considered. C_{Ca} and δC_{Ca} have therefore a uniform value in the
 191 cross section of the discontinuity. They only depend on x_d ;
- 192 • the width of the crack $2h$ evolves in function of the amount of C_aCO_3 , ξ , created in
 193 the crack, i.e $2h(\xi)$. The physical meaning being that the amount of C_aCO_3 created
 194 decreases the crack width value;
- 195 • the fluid velocity follows Darcy's Law such as $\mathbf{v}_w^f = -k_d(h)\nabla p_w$ where $k_d(h)$ is the
 196 crack permeability depending on the crack width h through the cubic law [22] and
 197 ∇p_w is the pressure gradient imposed during the computation;
- 198 • the transport by diffusion is induced by Fick's Law such as $\mathbf{J}_{Ca}^f = -\Phi^f D^f(h)\nabla C_{Ca}$
 199 where $D^f(h)$ is the diffusion coefficient in the crack depending on the crack width h .

200 4.2. Analytical model relating the width of the crack $2h$ and the amount of C_aCO_3

201 In order to relate the width of the crack $2h$ to the amount of C_aCO_3 , ξ , an analytical
 202 model is suggested hereafter.

As suggested in [6], we assume that the updated crack width $2h$ taking into account the
 layer of calcite e formed during the sealing process is

$$2h = 2h_0 - 2e, \quad (24)$$

203 where $2h_0$ is the initial width of the crack.

204 According to [6], the layer calcite e can be written as follows:

$$e = \lambda V_\xi \bar{C}_{Ca} \bar{C}_{CO_3}, \quad (25)$$

205 where λ is a fitting parameter depending on the crack characteristics and V_ξ the molar
 206 volume of calcite ($37 \text{ cm}^3.\text{mol}^{-1}$). \bar{C}_{Ca} and \bar{C}_{CO_3} are the mean values of C_{Ca} and C_{CO_3} in
 207 the crack.

208 4.3. Computational aspects for the coupling term

The first and last integrals in eqn. 23 are such as:

$$\int_{\Omega_d} \delta C_{Ca} \frac{\partial \Phi^f C_{Ca}}{\partial t} d\Omega = \int_{\Gamma_d} \int_{-h(\xi)}^{h(\xi)} \delta C_{Ca} \frac{\partial \Phi^f C_{Ca}}{\partial t} dy_d d\Gamma = \int_{\Gamma_d} \delta C_{Ca} 2h(\xi) \frac{\partial \Phi^f C_{Ca}}{\partial t} d\Gamma \quad (26)$$

$$\int_{\Omega_d} \delta C_{Ca} \frac{\partial \xi}{\partial t} d\Omega = \int_{\Gamma_d} \int_{-h(\xi)}^{h(\xi)} \delta C_{Ca} \frac{\partial \xi}{\partial t} dy_d d\Gamma = \int_{\Gamma_d} \delta C_{Ca} 2h(\xi) \frac{\partial \xi}{\partial t} d\Gamma \quad (27)$$

For the second term in eqn. 23, we have

$$\begin{aligned} \int_{\Omega_d} \nabla(\delta C_{Ca}) \cdot (\Phi^f C_{Ca} \mathbf{v}_w^f) d\Omega &= - \int_{\Gamma_d} \int_{-h(\xi)}^{h(\xi)} \nabla(\delta C_{Ca}) \cdot (\Phi^f C_{Ca} k_d(h) \nabla p_w) dy_d d\Gamma \\ &= - \int_{\Gamma_d} \int_{-h(\xi)}^{h(\xi)} (\Phi^f C_{Ca} k_d(h)) \left(\frac{\partial \delta C_{Ca}}{\partial x_d} \frac{\partial p_w}{\partial x_d} + \frac{\partial \delta C_{Ca}}{\partial y_d} \frac{\partial p_w}{\partial y_d} \right) dy_d d\Gamma \end{aligned} \quad (28)$$

Because the (virtual) calcium ions concentration is supposed to be dependent only in x_d , its derivative in relation with y_d vanishes. Consequently, eqn. 28 becomes:

$$\int_{\Omega_d} \nabla(\delta C_{Ca}) \cdot (\Phi^f C_{Ca} \mathbf{v}_w^f) d\Omega = - \int_{\Gamma_d} \Phi^f C_{Ca} k_d(h) 2h(\xi) \frac{\partial \delta C_{Ca}}{\partial x_d} \frac{\partial p_w}{\partial x_d} d\Gamma \quad (29)$$

For the third term in eqn. 23, we have

$$\begin{aligned} \int_{\Omega_d} \nabla(\delta C_{Ca}) \cdot (\mathbf{J}_{Ca}^f) d\Omega &= - \int_{\Gamma_d} \int_{-h(\xi)}^{h(\xi)} \nabla(\delta C_{Ca}) \cdot (\Phi^f D^f(h) \nabla C_{Ca}) dy_d d\Gamma \\ &= - \int_{\Gamma_d} \int_{-h(\xi)}^{h(\xi)} \Phi^f D^f(h) \left(\frac{\partial \delta C_{Ca}}{\partial x_d} \frac{\partial C_{Ca}}{\partial x_d} + \frac{\partial \delta C_{Ca}}{\partial y_d} \frac{\partial C_{Ca}}{\partial y_d} \right) dy_d d\Gamma \end{aligned} \quad (30)$$

As mentioned, the (virtual) calcium ions concentration derivative in relation with y_d vanishes. Consequently, eqn. 30 becomes:

$$\int_{\Omega_d} \nabla(\delta C_{Ca}) \cdot (\mathbf{J}_{Ca}^f) d\Omega = - \int_{\Gamma_d} \Phi^f D^f(h) 2h(\xi) \frac{\partial \delta C_{Ca}}{\partial x_d} \frac{\partial C_{Ca}}{\partial x_d} d\Gamma \quad (31)$$

Injecting eqn. 26, 27, 29 and 31 in eqn. 23 yields to the expression of the coupling term:

$$\begin{aligned} \int_{\Gamma_d} \delta C_{Ca} J_{\Gamma_d} d\Gamma &= - \int_{\Gamma_d} \delta C_{Ca} 2h(\xi) \frac{\partial \Phi^f C_{Ca}}{\partial t} d\Gamma - \int_{\Gamma_d} \Phi^f C_{Ca} k_d(h) 2h(\xi) \frac{\partial \delta C_{Ca}}{\partial x_d} \frac{\partial p_w}{\partial x_d} d\Gamma \\ &\quad - \int_{\Gamma_d} \Phi^f D^f(h) 2h(\xi) \frac{\partial \delta C_{Ca}}{\partial x_d} \frac{\partial C_{Ca}}{\partial x_d} d\Gamma - \int_{\Gamma_d} \delta C_{Ca} 2h(\xi) \frac{\partial \xi}{\partial t} d\Gamma \end{aligned} \quad (32)$$

Finally, combining eqn. 32 and eqn. 11 leads to:

$$\begin{aligned} &\int_{\Omega} \delta C_{Ca} \frac{\partial \Phi^m C_{Ca}}{\partial t} d\Omega - \int_{\Omega} \nabla(\delta C_{Ca}) \cdot \mathbf{J}_{Ca}^m d\Omega + \int_{\partial\Omega_{J_{Ca}^m}} \delta C_{Ca} \bar{J}_{Ca}^m d\partial\Omega + \int_{\Gamma_d} \delta C_{Ca} 2h(\xi) \frac{\partial \Phi^f C_{Ca}}{\partial t} d\Gamma \\ &+ \int_{\Gamma_d} \Phi^f C_{Ca} k_d(h) 2h(\xi) \frac{\partial \delta C_{Ca}}{\partial x_d} \frac{\partial p_w}{\partial x_d} d\Gamma + \int_{\Gamma_d} \Phi^f D^f(h) 2h(\xi) \frac{\partial \delta C_{Ca}}{\partial x_d} \frac{\partial C_{Ca}}{\partial x_d} d\Gamma + \int_{\Gamma_d} \delta C_{Ca} 2h(\xi) \frac{\partial \xi}{\partial t} d\Gamma \\ &= \int_{\Omega} \delta C_{Ca} \Phi^m \varphi_{Ca_s} d\Omega. \end{aligned} \quad (33)$$

Eqn. 33 and 22 represent the equations of the problem to be solved in terms of C_{Ca} and C_{CO_3} .

Having in hand, the weak form of the problem equations, we now turn to the discretization of the concentration fields C_{Ca} and C_{CO_3} .

5. FE discretization of the governing equations

5.1. Continuous form of the concentration fields

5.1.1. Calcium ions concentration field

As mentioned the fluid flow of calcium ions normal to the discontinuity has to be discontinuous. Because the fluid flow is related to the calcium concentration gradient through Darcy's Law, the gradient of the calcium ions concentration normal to the discontinuity has to be discontinuous. Consequently, the enrichment function of the interpolation of the calcium ions concentration field must be such as the calcium ions concentration itself is continuous but has a discontinuous gradient in the normal direction. To fulfill this requirement, a weak discontinuity is introduced in the calcium ions concentration field through the EAS method [16]. In this sense, we consider both the calcium ions concentration and the virtual

224 calcium ions concentration fields decomposed into a regular and an enhanced part. This
 225 assumption gives for the calcium ions concentration field

$$C_{Ca} = \underbrace{\bar{C}_{Ca}}_{\text{regular}} + \underbrace{\tilde{C}_{Ca}}_{\text{enhanced}}, \quad (34)$$

and for the virtual calcium ions concentration field

$$\delta C_{Ca} = \underbrace{\delta \bar{C}_{Ca}}_{\text{regular}} + \underbrace{\delta \tilde{C}_{Ca}}_{\text{enhanced}}. \quad (35)$$

226 As in [16], we refer to \tilde{C}_{Ca} and $\delta \tilde{C}_{Ca}$ as the enhanced parts of the calcium ions concen-
 227 tration fields. The notation $(\tilde{\bullet})$ refers to the weak discontinuity.

The enrichment function \tilde{C}_{Ca} satisfying the condition - continuous concentration field and discontinuous gradient in normal direction - is based upon a weak discontinuity such as:

$$\tilde{C}_{Ca} = \Theta \mathbf{n}_{\Gamma_d} \cdot (\mathbf{x} - \boldsymbol{\xi}) \quad (36)$$

228 where $\boldsymbol{\xi}$ represents the position of Γ_d and Θ an unidentified shape function. The product
 229 $\mathbf{n}_{\Gamma_d} \cdot (\mathbf{x} - \boldsymbol{\xi})$ is called the signed distance function, $\Sigma_{\Gamma_d}(\mathbf{x})$. This function is plotted in Fig.
 230 3 in the context of 1D problem. Note that when \mathbf{x} is equal to $\boldsymbol{\xi}$ (in other words when we
 231 are on the discontinuity Γ_d), \tilde{C}_{Ca} is equal to zero thus the calcium ions concentration is
 232 continuous through the discontinuity. A signed distance function is also considered in [14]
 233 and [23] for the meso-scale modelling of a two-phase quasi-brittle material and a two-phase
 234 poro-elastic material, respectively. Both authors suggest a model written in the E-FEM
 235 framework. In the context of the X-FEM, the absolute value of the signed distance function
 236 is regarded in [17] and [18] for the modelling of hydraulic crack and in [24] to represent
 237 complex microstructure geometries.

Considering the gradient of $\Sigma_{\Gamma_d}(\mathbf{x})$ yield (see [23]):

$$\nabla(\Sigma_{\Gamma_d}(\mathbf{x})) = \begin{pmatrix} n_1 \\ n_2 \end{pmatrix} = \mathbf{n}_{\Gamma_d}. \quad (37)$$

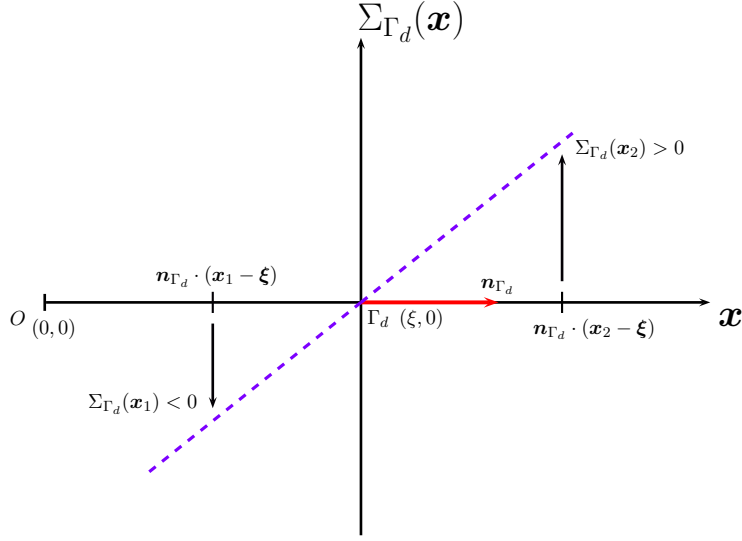


Figure 3: 1D plot of the signed distance function $\Sigma_{\Gamma_d}(\mathbf{x})$

Finally, eqn. 37 gives for the gradient of \tilde{C}_{Ca} the following form:

$$\nabla \tilde{C}_{Ca} = \Theta \begin{pmatrix} n_1 \\ n_2 \end{pmatrix} = \Theta \mathbf{n}_{\Gamma_d}. \quad (38)$$

238 As it will be explained after, eqn. 38 satisfies the discontinuous requirement in the
 239 gradient normal direction.

240 5.1.2. Carbonate ions concentration field

241 For the carbonate ions concentration field, there is no need for an enhanced function.
 242 Only the regular part is required such as:

$$C_{CO_3} = \underbrace{\bar{C}_{CO_3}}_{\text{regular}}. \quad (39)$$

243 5.2. Discrete form of the concentration fields

244 After presenting the continuous forms of the concentration fields and more particularly
 245 the form of the enhanced calcium concentration field, we now turn to their discrete expres-
 246 sions.

247 *5.2.1. Calcium ions concentration field*

248 Starting from eqn. 34 and 35, the discrete forms of C_{Ca} and δC_{Ca} labeled as C_{Ca}^h and
 249 δC_{Ca}^h are

$$C_{Ca}^h = \mathbf{N}_{Ca} \bar{\mathbf{C}}_{Ca}^h + M_{Ca} \tilde{C}_{Ca}^h, \quad (40)$$

and

$$\delta C_{Ca}^h = \mathbf{N}_{Ca} \delta \bar{\mathbf{C}}_{Ca}^h + M_{Ca} \delta \tilde{C}_{Ca}^h, \quad (41)$$

250 where \mathbf{N}_{Ca} is a row vector containing the standard shape functions, $\bar{\mathbf{C}}_{Ca}^h$ is a column vector
 251 containing the regular calcium ions concentration unknowns. M_{Ca} is a scalar value cor-
 252 responding to the discrete form of the enhanced function (eqn. 36) and \tilde{C}_{Ca}^h is a scalar
 253 value corresponding to the enhanced parameter. This parameter is computed during the
 254 resolution process only for the elements containing a crack.

255 Following the idea presented in [23] and eqn. 36, the form of M_{Ca} is such as:

$$M_{Ca} = \begin{cases} M_{Ca}^{\oplus} = \Theta^{\oplus} \mathbf{n} \cdot (\mathbf{x}^{\oplus} - \boldsymbol{\xi}) = \frac{V^{\ominus}}{V} \mathbf{n} \cdot (\mathbf{x}^{\oplus} - \boldsymbol{\xi}) & \text{in } \Omega_e^{\oplus} \\ M_{Ca}^{\ominus} = \Theta^{\ominus} \mathbf{n} \cdot (\mathbf{x}^{\ominus} - \boldsymbol{\xi}) = -\frac{V^{\oplus}}{V} \mathbf{n} \cdot (\mathbf{x}^{\ominus} - \boldsymbol{\xi}) & \text{in } \Omega_e^{\ominus} \end{cases}, \quad (42)$$

256 where V^{\oplus} and V^{\ominus} are the volume of Ω_e^{\oplus} and Ω_e^{\ominus} , respectively.

257 Fig. 4 plots the enhanced function M_{Ca} in the 1D case. We have arbitrarily chosen V^{\ominus}
 258 equals to 0.3, V^{\oplus} to 0.7 and ξ to 0.3. The section and the length of the 1D domain are equal
 259 to 1.

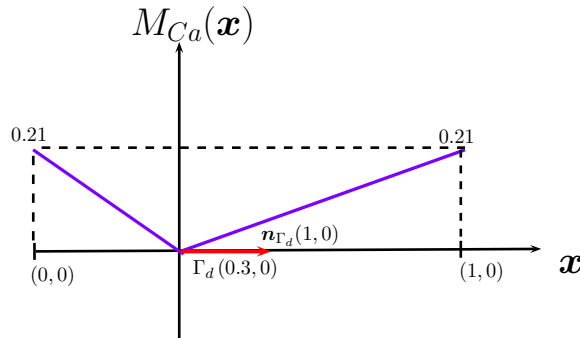


Figure 4: 1D plot of the enhanced function M_{Ca}

260 Consequently the gradients of C_{Ca}^h and δC_{Ca}^h are

$$\nabla C_{Ca}^h = \mathbf{B}_{Ca} \bar{\mathbf{C}}_{Ca}^h + \mathbf{G}_{Ca} \tilde{\mathbf{C}}_{Ca}^h, \quad (43)$$

and

$$\nabla \delta C_{Ca}^h = \mathbf{B}_{Ca} \delta \bar{\mathbf{C}}_{Ca}^h + \mathbf{G}_{Ca} \delta \tilde{\mathbf{C}}_{Ca}^h, \quad (44)$$

261 where \mathbf{B}_{Ca} is a matrix containing the derivatives of the shape functions \mathbf{N}_{Ca} and \mathbf{G}_{Ca} is a
262 vector containing the derivative of M_{Ca} . \mathbf{G}_{Ca} corresponds to the discrete form of eqn. 38.

The form of \mathbf{G}_{Ca} is such as

$$\mathbf{G}_{Ca} = \begin{cases} \mathbf{G}_{Ca}^{\oplus} = \Theta^{\oplus} \mathbf{H} = \frac{V^{\ominus}}{V} \mathbf{H} & \text{in } \Omega_e^{\oplus} \\ \mathbf{G}_{Ca}^{\ominus} = \Theta^{\ominus} \mathbf{H} = -\frac{V^{\oplus}}{V} \mathbf{H} & \text{in } \Omega_e^{\ominus} \end{cases} \quad (45)$$

with

$$\mathbf{H} = \begin{pmatrix} n_1 \\ n_2 \end{pmatrix}. \quad (46)$$

263 Fig. 5 plots the enhanced function \mathbf{G}_{Ca} in the 1D case and illustrates the discontinuous
264 requirement in the normal direction when passing through Γ_d .

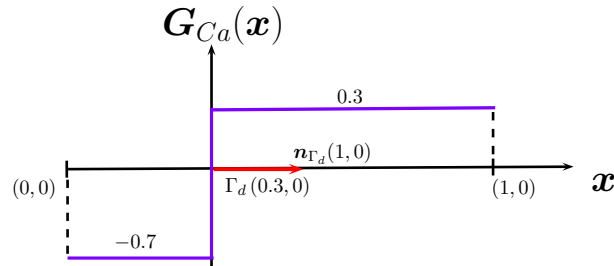


Figure 5: 1D plot of the enhanced function \mathbf{G}_{Ca}

265 5.2.2. Carbonate ions concentration field

266 The discrete form of the carbonate ions concentration field is such as:

$$C_{CO_3}^h = \mathbf{N}_{CO_3} \bar{\mathbf{C}}_{CO_3}^h \quad (47)$$

and

$$\delta C_{CO_3}^h = \mathbf{N}_{CO_3} \delta \bar{\mathbf{C}}_{CO_3}^h, \quad (48)$$

267 where \mathbf{N}_{CO_3} is a row vector containing the standard shape functions and $\bar{\mathbf{C}}_{CO_3}^h$ a column
 268 vector containing the regular carbonate ions concentration unknowns.

269 Consequently the gradients of $C_{CO_3}^h$ and $\delta C_{CO_3}^h$ are:

$$\nabla C_{CO_3}^h = \mathbf{B}_{CO_3} \bar{\mathbf{C}}_{CO_3}^h \quad (49)$$

and

$$\nabla \delta C_{CO_3}^h = \mathbf{B}_{CO_3} \delta \bar{\mathbf{C}}_{CO_3}^h, \quad (50)$$

270 where \mathbf{B}_{CO_3} is a matrix containing the derivatives of the shape functions \mathbf{N}_{CO_3} .

271 5.3. Discrete form of the governing equations

Combining eqn. 40, 41, 43, 44 and eqn. 33 and considering the fact that the weak form of the equations has to hold for all kinematically admissible test functions $\delta \bar{\mathbf{C}}_{Ca}^h$ and $\delta \tilde{\mathbf{C}}_{Ca}^h$ yield:

$$\begin{cases} M_{\bar{\mathbf{C}}_a \bar{\mathbf{C}}_a} \dot{\bar{\mathbf{C}}}_{Ca}^h + M_{\tilde{\mathbf{C}}_a \tilde{\mathbf{C}}_a} \dot{\tilde{\mathbf{C}}}_{Ca}^h + \mathbf{H}_{\bar{\mathbf{C}}_a \bar{\mathbf{C}}_a} \bar{\mathbf{C}}_{Ca}^h + \mathbf{H}_{\tilde{\mathbf{C}}_a \tilde{\mathbf{C}}_a} \tilde{\mathbf{C}}_{Ca}^h - \mathbf{F}_{int, \bar{\mathbf{C}}_a} = \mathbf{F}_{ext, \bar{\mathbf{C}}_a} \\ M_{\bar{\mathbf{C}}_a \tilde{\mathbf{C}}_a}^T \dot{\bar{\mathbf{C}}}_{Ca}^h + M_{\tilde{\mathbf{C}}_a \bar{\mathbf{C}}_a} \dot{\tilde{\mathbf{C}}}_{Ca}^h + \mathbf{H}_{\bar{\mathbf{C}}_a \tilde{\mathbf{C}}_a}^T \bar{\mathbf{C}}_{Ca}^h + \mathbf{H}_{\tilde{\mathbf{C}}_a \bar{\mathbf{C}}_a} \tilde{\mathbf{C}}_{Ca}^h - \mathbf{F}_{int, \tilde{\mathbf{C}}_a} = \mathbf{F}_{ext, \tilde{\mathbf{C}}_a} \end{cases} \quad (51)$$

Combining eqn. 47, 48, 49, 50 and eqn. 22, assuming that C_{CO_3} and δC_{CO_3} depend only on x_d (see the arguments before) and considering the fact that the weak form of the equation has to hold for all kinematically admissible test functions $\delta \bar{\mathbf{C}}_{CO_3}^h$ lead to:

$$\mathbf{F}_{int, \bar{\mathbf{C}}_{CO_3}} = 0 \quad (52)$$

272 The definition of the matrix and vector coefficients are given in Appendix A.

273 5.4. Linearization of the governing equations

274 In a first time, we note for the k th iteration at the $n + 1$ time step :

$$\begin{aligned} \mathbf{R}_{n+1}^{(k)} &= \frac{1}{\Delta t} M_{\bar{\mathbf{C}}_a \bar{\mathbf{C}}_a} |_{n+1}^{(k)} \Delta \bar{\mathbf{C}}_{Ca}^h |_{n+1}^{(k)} + \frac{1}{\Delta t} M_{\tilde{\mathbf{C}}_a \tilde{\mathbf{C}}_a} |_{n+1}^{(k)} \Delta \tilde{\mathbf{C}}_{Ca}^h |_{n+1}^{(k)} + \mathbf{H}_{\bar{\mathbf{C}}_a \bar{\mathbf{C}}_a} |_{n+1}^{(k)} \bar{\mathbf{C}}_{Ca}^h |_{n+1}^{(k)} \\ &\quad + \mathbf{H}_{\tilde{\mathbf{C}}_a \tilde{\mathbf{C}}_a} |_{n+1}^{(k)} \tilde{\mathbf{C}}_{Ca}^h |_{n+1}^{(k)} - \mathbf{F}_{int, \bar{\mathbf{C}}_a} |_{n+1}^{(k)} - \mathbf{F}_{ext, \bar{\mathbf{C}}_a} |_{n+1}, \end{aligned} \quad (53)$$

$$\begin{aligned}
h_{n+1}^{(k)} &= \frac{1}{\Delta t} \mathbf{M}_{\bar{\mathbf{C}}_a \tilde{\mathbf{C}}_a}^T |_{n+1}^{(k)} \Delta \bar{\mathbf{C}}_{Ca}^h |_{n+1}^{(k)} + \frac{1}{\Delta t} \mathbf{M}_{\tilde{\mathbf{C}}_a \bar{\mathbf{C}}_a} |_{n+1}^{(k)} \Delta \tilde{\mathbf{C}}_{Ca}^h |_{n+1}^{(k)} + \mathbf{H}_{\bar{\mathbf{C}}_a \tilde{\mathbf{C}}_a}^T |_{n+1}^{(k)} \bar{\mathbf{C}}_{Ca}^h |_{n+1}^{(k)} \\
&+ \mathbf{H}_{\tilde{\mathbf{C}}_a \bar{\mathbf{C}}_a} |_{n+1}^{(k)} \tilde{\mathbf{C}}_{Ca}^h |_{n+1}^{(k)} - \mathbf{F}_{int, \bar{\mathbf{C}}_a} |_{n+1}^{(k)} - \mathbf{F}_{ext, \bar{\mathbf{C}}_a} |_{n+1}, \tag{54}
\end{aligned}$$

275 where the Newmark integration scheme for time dependent terms has been considered,
and

$$\mathbf{F}_{int, \bar{\mathbf{C}}_{CO_3}} |_{n+1}^{(k)} = 0. \tag{55}$$

276 Although several schemes are possible, here we consider determinating $\Delta \bar{\mathbf{C}}_{Ca}^h |_{n+1}^{(k+1)}$,
277 $\Delta \tilde{\mathbf{C}}_{Ca}^h |_{n+1}^{(k+1)}$ and $\Delta \bar{\mathbf{C}}_{CO_3}^h |_{n+1}^{(k+1)}$ by linearizing $\mathbf{R}_{n+1}^{(k)}$, $h_{n+1}^{(k)}$ and $\mathbf{F}_{int, \bar{\mathbf{C}}_{CO_3}} |_{n+1}^{(k)}$ about the cur-
278 rent state, defined by $\bar{\mathbf{C}}_{Ca}^h |_{n+1}^{(k)}$, $\tilde{\mathbf{C}}_{Ca}^h |_{n+1}^{(k)}$ and $\bar{\mathbf{C}}_{CO_3}^h |_{n+1}^{(k)}$.

279 Consequently, the linearization of eqn. 53, 54 and 55 leads to:

$$\begin{aligned}
-\mathbf{R}_{n+1}^{(k)} &= \left[\frac{1}{\Delta t} \mathbf{M}_{\bar{\mathbf{C}}_a \tilde{\mathbf{C}}_a} + \mathbf{H}_{\bar{\mathbf{C}}_a \tilde{\mathbf{C}}_a} - \frac{\partial \mathbf{F}_{int, \bar{\mathbf{C}}_a}}{\partial \bar{\mathbf{C}}_{Ca}^h} \right] |_{n+1}^{(k)} \Delta \bar{\mathbf{C}}_{Ca}^h |_{n+1}^{(k+1)} \\
&+ \left[\frac{1}{\Delta t} \mathbf{M}_{\tilde{\mathbf{C}}_a \bar{\mathbf{C}}_a} + \mathbf{H}_{\tilde{\mathbf{C}}_a \bar{\mathbf{C}}_a} - \frac{\partial \mathbf{F}_{int, \tilde{\mathbf{C}}_a}}{\partial \tilde{\mathbf{C}}_{Ca}^h} \right] |_{n+1}^{(k)} \Delta \tilde{\mathbf{C}}_{Ca}^h |_{n+1}^{(k+1)} - \frac{\partial \mathbf{F}_{int, \bar{\mathbf{C}}_a}}{\partial \bar{\mathbf{C}}_{CO_3}^h} |_{n+1}^{(k)} \Delta \bar{\mathbf{C}}_{CO_3}^h |_{n+1}^{(k+1)}, \tag{56}
\end{aligned}$$

$$\begin{aligned}
-h_{n+1}^{(k)} &= \left[\frac{1}{\Delta t} \mathbf{M}_{\bar{\mathbf{C}}_a \tilde{\mathbf{C}}_a}^T + \mathbf{H}_{\bar{\mathbf{C}}_a \tilde{\mathbf{C}}_a}^T - \frac{\partial \mathbf{F}_{int, \tilde{\mathbf{C}}_a}}{\partial \bar{\mathbf{C}}_{Ca}^h} \right] |_{n+1}^{(k)} \Delta \bar{\mathbf{C}}_{Ca}^h |_{n+1}^{(k+1)} \\
&+ \left[\frac{1}{\Delta t} \mathbf{M}_{\tilde{\mathbf{C}}_a \bar{\mathbf{C}}_a} + \mathbf{H}_{\tilde{\mathbf{C}}_a \bar{\mathbf{C}}_a} - \frac{\partial \mathbf{F}_{int, \bar{\mathbf{C}}_a}}{\partial \tilde{\mathbf{C}}_{Ca}^h} \right] |_{n+1}^{(k)} \Delta \tilde{\mathbf{C}}_{Ca}^h |_{n+1}^{(k+1)} - \frac{\partial \mathbf{F}_{int, \tilde{\mathbf{C}}_a}}{\partial \bar{\mathbf{C}}_{CO_3}^h} |_{n+1}^{(k)} \Delta \bar{\mathbf{C}}_{CO_3}^h |_{n+1}^{(k+1)}, \tag{57}
\end{aligned}$$

and

$$\begin{aligned}
-\mathbf{F}_{int, \bar{\mathbf{C}}_{CO_3}} |_{n+1}^{(k)} &= \frac{\partial \mathbf{F}_{int, \bar{\mathbf{C}}_{CO_3}} |_{n+1}^{(k)}}{\partial \bar{\mathbf{C}}_{Ca}^h} \Delta \bar{\mathbf{C}}_{Ca}^h |_{n+1}^{(k+1)} + \frac{\partial \mathbf{F}_{int, \bar{\mathbf{C}}_{CO_3}} |_{n+1}^{(k)}}{\partial \tilde{\mathbf{C}}_{Ca}^h} \Delta \tilde{\mathbf{C}}_{Ca}^h |_{n+1}^{(k+1)} \\
&+ \frac{\partial \mathbf{F}_{int, \bar{\mathbf{C}}_{CO_3}} |_{n+1}^{(k)}}{\partial \bar{\mathbf{C}}_{CO_3}^h} \Delta \bar{\mathbf{C}}_{CO_3}^h |_{n+1}^{(k+1)}. \tag{58}
\end{aligned}$$

280 The form of the partial derivatives are given hereafter.

For eqn. 56, we have

$$\begin{aligned}
\frac{\partial \mathbf{F}_{int, \bar{\mathbf{C}}a}^{(k)}}{\partial \bar{\mathbf{C}}_{Ca}^h} \Big|_{n+1} &= -\frac{1}{\Delta t} \int_{\Gamma_d} \mathbf{N}_{Ca}^T 2h(\xi) \Phi^f \mathbf{N}_{Ca} d\Gamma - \int_{\Gamma_d} (\mathbf{B}_{Ca}^T \cdot \mathbf{t}_{\Gamma_d}) 2h(\xi) \Phi^f D^f(h) (\mathbf{t}_{\Gamma_d}^T \cdot \mathbf{B}_{Ca}) d\Gamma \\
&\quad - \int_{\Gamma_d} (\mathbf{B}_{Ca}^T \cdot \mathbf{t}_{\Gamma_d}) 2h(\xi) \Phi^f k_d(h) (\mathbf{t}_{\Gamma_d}^T \cdot \nabla p_w) \mathbf{N}_{Ca} d\Gamma \\
&\quad - \int_{\Gamma_d} \mathbf{N}_{Ca}^T 2h(\xi) K \mathbf{N}_{Ca} (\mathbf{N}_{CO_3} \bar{\mathbf{C}}_{CO_3}^h) d\Gamma, \tag{59}
\end{aligned}$$

$$\begin{aligned}
\frac{\partial \mathbf{F}_{int, \tilde{\mathbf{C}}a}^{(k)}}{\partial \tilde{\mathbf{C}}_{Ca}^h} \Big|_{n+1} &= -\frac{1}{\Delta t} \int_{\Gamma_d} \mathbf{N}_{Ca}^T 2h(\xi) \Phi^f M_{Ca} d\Gamma - \int_{\Gamma_d} (\mathbf{B}_{Ca}^T \cdot \mathbf{t}_{\Gamma_d}) 2h(\xi) \Phi^f D^f(h) (\mathbf{t}_{\Gamma_d}^T \cdot \mathbf{G}_{Ca}) d\Gamma \\
&\quad - \int_{\Gamma_d} (\mathbf{B}_{Ca}^T \cdot \mathbf{t}_{\Gamma_d}) 2h(\xi) \Phi^f k_d(h) (\mathbf{t}_{\Gamma_d}^T \cdot \nabla p_w) M_{Ca} d\Gamma \\
&\quad - \int_{\Gamma_d} \mathbf{N}_{Ca}^T 2h(\xi) K M_{Ca} (\mathbf{N}_{CO_3} \tilde{\mathbf{C}}_{CO_3}^h) d\Gamma, \tag{60}
\end{aligned}$$

and

$$\frac{\partial \mathbf{F}_{int, \bar{\mathbf{C}}a}^{(k)}}{\partial \bar{\mathbf{C}}_{CO_3}^h} \Big|_{n+1} = - \int_{\Gamma_d} \mathbf{N}_{Ca}^T 2h(\xi) K (\mathbf{N}_{Ca} \bar{\mathbf{C}}_{Ca}^h + M_{Ca} \tilde{\mathbf{C}}_{Ca}^h) \mathbf{N}_{CO_3} d\Gamma. \tag{61}$$

For eqn. 57, we have

$$\begin{aligned}
\frac{\partial \mathbf{F}_{int, \tilde{\mathbf{C}}a}^{(k)}}{\partial \tilde{\mathbf{C}}_{Ca}^h} \Big|_{n+1} &= -\frac{1}{\Delta t} \int_{\Gamma_d} M_{Ca}^T 2h(\xi) \Phi^f \mathbf{N}_{Ca} d\Gamma - \int_{\Gamma_d} (\mathbf{G}_{Ca}^T \cdot \mathbf{t}_{\Gamma_d}) 2h(\xi) \Phi^f D^f(h) (\mathbf{t}_{\Gamma_d}^T \cdot \mathbf{B}_{Ca}) d\Gamma \\
&\quad - \int_{\Gamma_d} (\mathbf{G}_{Ca}^T \cdot \mathbf{t}_{\Gamma_d}) 2h(\xi) \Phi^f k_d(h) (\mathbf{t}_{\Gamma_d}^T \cdot \nabla p_w) \mathbf{N}_{Ca} d\Gamma \\
&\quad - \int_{\Gamma_d} M_{Ca}^T 2h(\xi) K \mathbf{N}_{Ca} (\mathbf{N}_{CO_3} \tilde{\mathbf{C}}_{CO_3}^h) d\Gamma, \tag{62}
\end{aligned}$$

$$\begin{aligned}
\frac{\partial \mathbf{F}_{int, \tilde{\mathbf{C}}a}^{(k)}}{\partial \tilde{\mathbf{C}}_{Ca}^h} \Big|_{n+1} &= -\frac{1}{\Delta t} \int_{\Gamma_d} M_{Ca}^T 2h(\xi) \Phi^f M_{Ca} d\Gamma - \int_{\Gamma_d} (\mathbf{G}_{Ca}^T \cdot \mathbf{t}_{\Gamma_d}) 2h(\xi) \Phi^f D^f(h) (\mathbf{t}_{\Gamma_d}^T \cdot \mathbf{G}_{Ca}) d\Gamma \\
&\quad - \int_{\Gamma_d} (\mathbf{G}_{Ca}^T \cdot \mathbf{t}_{\Gamma_d}) 2h(\xi) \Phi^f k_d(h) (\mathbf{t}_{\Gamma_d}^T \cdot \nabla p_w) M_{Ca} d\Gamma \\
&\quad - \int_{\Gamma_d} M_{Ca}^T 2h(\xi) K M_{Ca} (\mathbf{N}_{CO_3} \tilde{\mathbf{C}}_{CO_3}^h) d\Gamma, \tag{63}
\end{aligned}$$

and

$$\frac{\partial \mathbf{F}_{int, \tilde{\mathbf{C}}_a}^{(k)}}{\partial \tilde{\mathbf{C}}_{CO_3}^h} \Big|_{n+1} = - \int_{\Gamma_d} M_{Ca}^T 2h(\xi) K (\mathbf{N}_{Ca} \tilde{\mathbf{C}}_{Ca}^h + M_{Ca} \tilde{\mathbf{C}}_{Ca}^h) \mathbf{N}_{CO_3} d\Gamma. \quad (64)$$

283

For eqn. 58, we have

$$\frac{\partial \mathbf{F}_{int, \tilde{\mathbf{C}}_{CO_3}}^{(k)}}{\partial \tilde{\mathbf{C}}_{Ca}^h} \Big|_{n+1} = \int_{\Gamma_d} \mathbf{N}_{CO_3}^T 2h(\xi) K \mathbf{N}_{Ca} (\mathbf{N}_{CO_3} \tilde{\mathbf{C}}_{CO_3}^h) d\Gamma, \quad (65)$$

$$\frac{\partial \mathbf{F}_{int, \tilde{\mathbf{C}}_{CO_3}}^{(k)}}{\partial \tilde{\mathbf{C}}_{Ca}^h} \Big|_{n+1} = \int_{\Gamma_d} \mathbf{N}_{CO_3}^T 2h(\xi) K M_{Ca} (\mathbf{N}_{CO_3} \tilde{\mathbf{C}}_{CO_3}^h) d\Gamma, \quad (66)$$

and

$$\begin{aligned} \frac{\partial \mathbf{F}_{int, \tilde{\mathbf{C}}_{CO_3}}^{(k)}}{\partial \tilde{\mathbf{C}}_{CO_3}^h} \Big|_{n+1} &= \frac{1}{\Delta t} \int_{\Gamma_d} \mathbf{N}_{CO_3}^T 2h(\xi) \Phi^f \mathbf{N}_{CO_3} d\Gamma \\ &+ \int_{\Gamma_d} (\mathbf{B}_{CO_3}^T \cdot \mathbf{t}_{\Gamma_d}) 2h(\xi) \Phi^f k_d(h) (\mathbf{t}_{\Gamma_d}^T \cdot \nabla p_w) \mathbf{N}_{CO_3} d\Gamma \\ &+ \int_{\Gamma_d} \mathbf{N}_{CO_3}^T 2h(\xi) K (\mathbf{N}_{Ca} \tilde{\mathbf{C}}_{Ca}^h + M_{Ca} \tilde{\mathbf{C}}_{Ca}^h) \mathbf{N}_{CO_3} d\Gamma. \end{aligned} \quad (67)$$

284

5.5. Numerical solving strategy

From eqn. 58, we can establish the expression of $\Delta \tilde{\mathbf{C}}_{CO_3}^h \Big|_{n+1}^{(k+1)}$ in function of $\Delta \tilde{\mathbf{C}}_{Ca}^h \Big|_{n+1}^{(k+1)}$ and $\Delta \tilde{\mathbf{C}}_{Ca}^h \Big|_{n+1}^{(k+1)}$ such as:

$$\begin{aligned} \Delta \tilde{\mathbf{C}}_{CO_3}^h \Big|_{n+1}^{(k+1)} &= \left[\frac{\partial \mathbf{F}_{int, \tilde{\mathbf{C}}_{CO_3}}^{(k)}}{\partial \tilde{\mathbf{C}}_{CO_3}^h} \Big|_{n+1} \right]^{-1} \left[- \mathbf{F}_{int, \tilde{\mathbf{C}}_{CO_3}} \Big|_{n+1}^{(k)} - \frac{\partial \mathbf{F}_{int, \tilde{\mathbf{C}}_{CO_3}}^{(k)}}{\partial \tilde{\mathbf{C}}_{Ca}^h} \Big|_{n+1} \Delta \tilde{\mathbf{C}}_{Ca}^h \Big|_{n+1}^{(k+1)} \right. \\ &\quad \left. - \frac{\partial \mathbf{F}_{int, \tilde{\mathbf{C}}_{CO_3}}^{(k)}}{\partial \tilde{\mathbf{C}}_{Ca}^h} \Big|_{n+1} \Delta \tilde{\mathbf{C}}_{Ca}^h \Big|_{n+1}^{(k+1)} \right]. \end{aligned} \quad (68)$$

Combining eqn. 68 and eqn. 57 gives the expression of $\Delta \tilde{\mathbf{C}}_{Ca}^h \Big|_{n+1}^{(k+1)}$ in function of $\Delta \tilde{\mathbf{C}}_{Ca}^h \Big|_{n+1}^{(k+1)}$ such as:

$$\Delta \tilde{\mathbf{C}}_{Ca}^h \Big|_{n+1}^{(k+1)} = \left[A \Big|_{n+1}^{(k)} \right]^{-1} \left[- h_{n+1}^{(k)} - B \Big|_{n+1}^{(k)} - \mathbf{X} \Big|_{n+1}^{(k)} \Delta \tilde{\mathbf{C}}_{Ca}^h \Big|_{n+1}^{(k+1)} \right] \quad (69)$$

where, for sake of clarity, we note

$$\mathbf{X}|_{n+1}^{(k)} = \left[\frac{1}{\Delta t} \mathbf{M}_{\bar{\mathbf{C}}_a \bar{\mathbf{C}}_a}^T + \mathbf{H}_{\bar{\mathbf{C}}_a \bar{\mathbf{C}}_a}^T - \frac{\partial \mathbf{F}_{int, \bar{\mathbf{C}}_a}}{\partial \bar{\mathbf{C}}_{C_a}^h} + \frac{\partial \mathbf{F}_{int, \bar{\mathbf{C}}_a}}{\partial \bar{\mathbf{C}}_{CO_3}^h} \left[\frac{\partial \mathbf{F}_{int, \bar{\mathbf{C}}_{CO_3}}}{\partial \bar{\mathbf{C}}_{CO_3}^h} \right]^{-1} \frac{\partial \mathbf{F}_{int, \bar{\mathbf{C}}_{CO_3}}}{\partial \bar{\mathbf{C}}_{C_a}^h} \right] \Big|_{n+1}^{(k)}, \quad (70)$$

$$\mathbf{A}|_{n+1}^{(k)} = \left[\frac{1}{\Delta t} \mathbf{M}_{\bar{\mathbf{C}}_a \bar{\mathbf{C}}_a} + \mathbf{H}_{\bar{\mathbf{C}}_a \bar{\mathbf{C}}_a} - \frac{\partial \mathbf{F}_{int, \bar{\mathbf{C}}_a}}{\partial \bar{\mathbf{C}}_{C_a}^h} + \frac{\partial \mathbf{F}_{int, \bar{\mathbf{C}}_a}}{\partial \bar{\mathbf{C}}_{CO_3}^h} \left[\frac{\partial \mathbf{F}_{int, \bar{\mathbf{C}}_{CO_3}}}{\partial \bar{\mathbf{C}}_{CO_3}^h} \right]^{-1} \frac{\partial \mathbf{F}_{int, \bar{\mathbf{C}}_{CO_3}}}{\partial \bar{\mathbf{C}}_{C_a}^h} \right] \Big|_{n+1}^{(k)}, \quad (71)$$

and

$$\mathbf{B}|_{n+1}^{(k)} = \frac{\partial \mathbf{F}_{int, \bar{\mathbf{C}}_a}}{\partial \bar{\mathbf{C}}_{CO_3}^h} \Big|_{n+1}^{(k)} \left[\frac{\partial \mathbf{F}_{int, \bar{\mathbf{C}}_{CO_3}}}{\partial \bar{\mathbf{C}}_{CO_3}^h} \Big|_{n+1}^{(k)} \right]^{-1} \mathbf{F}_{int, \bar{\mathbf{C}}_{CO_3}} \Big|_{n+1}^{(k)}. \quad (72)$$

We eventually obtain the problem to be solved in terms of $\Delta \bar{\mathbf{C}}_{C_a}^h|_{n+1}^{(k+1)}$ by combining eqn. 68 and 69 into eqn. 56 such as:

$$\hat{K}_{n+1}^{(k)} \Delta \bar{\mathbf{C}}_{C_a}^h|_{n+1}^{(k+1)} = \hat{F}_{n+1}^{(k)}, \quad (73)$$

285 where

$$\begin{aligned} \hat{K}_{n+1}^{(k)} &= \left[\frac{1}{\Delta t} \mathbf{M}_{\bar{\mathbf{C}}_a \bar{\mathbf{C}}_a} + \mathbf{H}_{\bar{\mathbf{C}}_a \bar{\mathbf{C}}_a} - \frac{\partial \mathbf{F}_{int, \bar{\mathbf{C}}_a}}{\partial \bar{\mathbf{C}}_{C_a}^h} - \left[\frac{1}{\Delta t} \mathbf{M}_{\bar{\mathbf{C}}_a \bar{\mathbf{C}}_a} + \mathbf{H}_{\bar{\mathbf{C}}_a \bar{\mathbf{C}}_a} - \frac{\partial \mathbf{F}_{int, \bar{\mathbf{C}}_a}}{\partial \bar{\mathbf{C}}_{C_a}^h} \right] [\mathbf{A}]^{-1} [\mathbf{X}] \right. \\ &\quad \left. + \frac{\partial \mathbf{F}_{int, \bar{\mathbf{C}}_a}}{\partial \bar{\mathbf{C}}_{CO_3}^h} \left[\frac{\partial \mathbf{F}_{int, \bar{\mathbf{C}}_{CO_3}}}{\partial \bar{\mathbf{C}}_{CO_3}^h} \right]^{-1} \frac{\partial \mathbf{F}_{int, \bar{\mathbf{C}}_{CO_3}}}{\partial \bar{\mathbf{C}}_{C_a}^h} - \frac{\partial \mathbf{F}_{int, \bar{\mathbf{C}}_a}}{\partial \bar{\mathbf{C}}_{CO_3}^h} \left[\frac{\partial \mathbf{F}_{int, \bar{\mathbf{C}}_{CO_3}}}{\partial \bar{\mathbf{C}}_{CO_3}^h} \right]^{-1} \frac{\partial \mathbf{F}_{int, \bar{\mathbf{C}}_{CO_3}}}{\partial \bar{\mathbf{C}}_{C_a}^h} [\mathbf{A}]^{-1} [\mathbf{X}] \right] \Big|_{n+1}^{(k)} \end{aligned} \quad (74)$$

and

$$\begin{aligned} \hat{F}_{n+1}^{(k)} &= -\mathbf{R}_{n+1}^{(k)} - \frac{\partial \mathbf{F}_{int, \bar{\mathbf{C}}_a}}{\partial \bar{\mathbf{C}}_{CO_3}^h} \Big|_{n+1}^{(k)} \left[\frac{\partial \mathbf{F}_{int, \bar{\mathbf{C}}_{CO_3}}}{\partial \bar{\mathbf{C}}_{CO_3}^h} \Big|_{n+1}^{(k)} \right]^{-1} \mathbf{F}_{int, \bar{\mathbf{C}}_{CO_3}} \Big|_{n+1}^{(k)} \\ &\quad + \left[\frac{1}{\Delta t} \mathbf{M}_{\bar{\mathbf{C}}_a \bar{\mathbf{C}}_a} + \mathbf{H}_{\bar{\mathbf{C}}_a \bar{\mathbf{C}}_a} - \frac{\partial \mathbf{F}_{int, \bar{\mathbf{C}}_a}}{\partial \bar{\mathbf{C}}_{C_a}^h} + \frac{\partial \mathbf{F}_{int, \bar{\mathbf{C}}_a}}{\partial \bar{\mathbf{C}}_{CO_3}^h} \left[\frac{\partial \mathbf{F}_{int, \bar{\mathbf{C}}_{CO_3}}}{\partial \bar{\mathbf{C}}_{CO_3}^h} \right]^{-1} \frac{\partial \mathbf{F}_{int, \bar{\mathbf{C}}_{CO_3}}}{\partial \bar{\mathbf{C}}_{C_a}^h} \right] \Big|_{n+1}^{(k)} \\ &\quad \left[\mathbf{A}|_{n+1}^{(k)} \right]^{-1} \left[\mathbf{h}_{n+1}^{(k)} + \mathbf{B}|_{n+1}^{(k)} \right]. \end{aligned} \quad (75)$$

286 Once $\Delta \bar{\mathbf{C}}_{C_a}^h|_{n+1}^{(k+1)}$ is known, $\Delta \bar{\mathbf{C}}_{C_a}^h|_{n+1}^{(k+1)}$ and $\Delta \bar{\mathbf{C}}_{CO_3}^h|_{n+1}^{(k+1)}$ can be computed through eqn.
287 69 and 68, respectively.

288 6. Conclusion

289 In this paper, we have suggested a numerical model for the healing process induced by
290 carbonation of a single crack in concrete structures. We have shown that careful consider-
291 ations concerning the transport equations are needed to have a realistic model. Chemical
292 reactions such as the calcite precipitation (resulting in the healing process), transport by
293 diffusion and permeation equations written in the porous matrix and in the crack and de-
294 pendence of the permeability and diffusivity coefficients on the calcite width are for instance
295 worth noting. In addition, considering the fact that there is a geometrical discontinuity Γ_d
296 embedded in the domain Ω , a mass transfer coupling between the porous bulk material sur-
297 rounding the crack and the crack itself arises. This mass transfer comes from the exchange
298 by diffusion of the calcium ions flow between the porous matrix surrounding the crack and
299 the crack itself. It is important to stress the fact that this coupling term arises naturally in
300 the weak form of the problem, since the crack is directly embedded in the mesh through the
301 E-FEM. This a serious advantage when the FE discretization is performed. Consequently,
302 concerning this term, an accurate FE approximation capable of accomodating the jump in
303 the normal direction of the calcium ions gradient has to be introduced. In this sense, a
304 weak discontinuity in the calcium ions concentration field for finite elements where the crack
305 is present is added in the framework of the EAS method. In addition, the solution proce-
306 dure for this class of problems retained in this paper is attractive since the framework of a
307 classical FE code is preserved. The enhanced parameters are just post-calculated. Finally,
308 the experimental validation of the model and its sensitivity analysis will be the object of a
309 forthcoming work. **In addition, healing process implies consideration of strength recovery
310 in the mechanical process. However the numerical model suggested in this paper only deals
311 with reactive transport equations. In this sense, no mechanical considerations are regarded
312 for the moment. One lead for introducing the healing process into a mechanical problem
313 could be to consider a (weak) coupled approach as done in [25]. The key point is to express
314 the mechanical properties (Young modulus for example) as a function of the crack opening
315 value, which depends itself on the calcite concentration. This idea is inspired by the work**

316 of [26] where the authors obtain the diffusion coefficient as a function of the crack opening
 317 in the context of chloride ingress problem.

318 7. Appendix A

319 The matrix and vector coefficients involved in system 51 and eqn. 52 are given hereafter.

$$\begin{aligned}
 \mathbf{M}_{\bar{C}_a \bar{C}_a} &= \int_{\Omega} \mathbf{N}_{C_a}^T \Phi^m \mathbf{N}_{C_a} d\Omega \\
 \mathbf{M}_{\bar{C}_a \tilde{C}_a} &= \int_{\Omega} \mathbf{N}_{C_a}^T \Phi^m M_{C_a} d\Omega \\
 \mathbf{M}_{\tilde{C}_a \bar{C}_a} &= \int_{\Omega} M_{C_a}^T \Phi^m M_{C_a} d\Omega \\
 \mathbf{H}_{\bar{C}_a \bar{C}_a} &= \int_{\Omega} \mathbf{B}_{C_a}^T \Phi^m D^m \mathbf{B}_{C_a} d\Omega \\
 \mathbf{H}_{\bar{C}_a \tilde{C}_a} &= \int_{\Omega} \mathbf{B}_{C_a}^T \Phi^m D^m \mathbf{G}_{C_a} d\Omega \\
 \mathbf{H}_{\tilde{C}_a \bar{C}_a} &= \int_{\Omega} \mathbf{G}_{C_a}^T \Phi^m D^m \mathbf{G}_{C_a} d\Omega \\
 \mathbf{F}_{int, \bar{C}_a} &= \int_{\Gamma_d} \mathbf{N}_{C_a}^T J_{\Gamma_d} d\Gamma \\
 &= - \int_{\Gamma_d} \mathbf{N}_{C_a}^T 2h(\xi) \Phi^f \mathbf{N}_{C_a} d\Gamma \dot{\bar{C}}_{C_a}^h \\
 &\quad - \int_{\Gamma_d} \mathbf{N}_{C_a}^T 2h(\xi) \Phi^f M_{C_a} d\Gamma \dot{\tilde{C}}_{C_a}^h \\
 &\quad - \int_{\Gamma_d} (\mathbf{B}_{C_a}^T \cdot \mathbf{t}_{\Gamma_d}) 2h(\xi) \Phi^f D^f(h) (\mathbf{t}_{\Gamma_d}^T \cdot \mathbf{B}_{C_a}) d\Gamma \bar{C}_{C_a}^h \\
 &\quad - \int_{\Gamma_d} (\mathbf{B}_{C_a}^T \cdot \mathbf{t}_{\Gamma_d}) 2h(\xi) \Phi^f D^f(h) (\mathbf{t}_{\Gamma_d}^T \cdot \mathbf{G}_{C_a}) d\Gamma \tilde{C}_{C_a}^h \\
 &\quad - \int_{\Gamma_d} (\mathbf{B}_{C_a}^T \cdot \mathbf{t}_{\Gamma_d}) 2h(\xi) \Phi^f k_d(h) (\mathbf{t}_{\Gamma_d}^T \cdot \nabla p_w) \mathbf{N}_{C_a} d\Gamma \bar{C}_{C_a}^h \\
 &\quad - \int_{\Gamma_d} (\mathbf{B}_{C_a}^T \cdot \mathbf{t}_{\Gamma_d}) 2h(\xi) \Phi^f k_d(h) (\mathbf{t}_{\Gamma_d}^T \cdot \nabla p_w) M_{C_a} d\Gamma \tilde{C}_{C_a}^h \\
 &\quad - \int_{\Gamma_d} \mathbf{N}_{C_a}^T 2h(\xi) \frac{\partial \xi}{\partial t} d\Gamma \\
 \mathbf{F}_{ext, \bar{C}_a} &= \int_{\Omega} \mathbf{N}_{C_a}^T \Phi^m \varphi_{C_{a_s}} d\Omega - \int_{\partial\Omega_{J_{C_a}^m}} \mathbf{N}_{C_a}^T \bar{J}_{C_a}^m d\partial\Omega
 \end{aligned} \tag{76}$$

$$\begin{aligned}
\mathbf{F}_{int, \tilde{C}a} &= \int_{\Gamma_d} M_{Ca}^T J_{\Gamma_d} d\Gamma \\
&= - \int_{\Gamma_d} M_{Ca}^T 2h(\xi) \Phi^f \mathbf{N}_{Ca} d\Gamma \dot{\tilde{C}}_{Ca}^h \\
&\quad - \int_{\Gamma_d} M_{Ca}^T 2h(\xi) \Phi^f M_{Ca} d\Gamma \dot{\tilde{C}}_{Ca}^h \\
&\quad - \int_{\Gamma_d} (\mathbf{G}_{Ca}^T \cdot \mathbf{t}_{\Gamma_d}) 2h(\xi) \Phi^f D^f(h) (\mathbf{t}_{\Gamma_d}^T \cdot \mathbf{B}_{Ca}) d\Gamma \bar{\tilde{C}}_{Ca}^h \\
&\quad - \int_{\Gamma_d} (\mathbf{G}_{Ca}^T \cdot \mathbf{t}_{\Gamma_d}) 2h(\xi) \Phi^f D^f(h) (\mathbf{t}_{\Gamma_d}^T \cdot \mathbf{G}_{Ca}) d\Gamma \tilde{C}_{Ca}^h \\
&\quad - \int_{\Gamma_d} (\mathbf{G}_{Ca}^T \cdot \mathbf{t}_{\Gamma_d}) 2h(\xi) \Phi^f k_d(h) (\mathbf{t}_{\Gamma_d}^T \cdot \nabla p_w) \mathbf{N}_{Ca} d\Gamma \bar{\tilde{C}}_{Ca}^h \\
&\quad - \int_{\Gamma_d} (\mathbf{G}_{Ca}^T \cdot \mathbf{t}_{\Gamma_d}) 2h(\xi) \Phi^f k_d(h) (\mathbf{t}_{\Gamma_d}^T \cdot \nabla p_w) M_{Ca} d\Gamma \tilde{C}_{Ca}^h \\
&\quad - \int_{\Gamma_d} M_{Ca}^T 2h(\xi) \frac{\partial \xi}{\partial t} d\Gamma \\
\mathbf{F}_{ext, \tilde{C}a} &= \int_{\Omega} M_{Ca}^T \Phi^m \varphi_{Ca_s} d\Omega - \int_{\partial\Omega_{J_{Ca}^m}} M_{Ca}^T \bar{J}_{Ca}^m d\partial\Omega
\end{aligned} \tag{77}$$

$$\begin{aligned}
\mathbf{F}_{int, \bar{C}CO_3} &= \int_{\Gamma_d} \mathbf{N}_{CO_3}^T 2h(\xi) \Phi^f \mathbf{N}_{CO_3} d\Gamma \dot{\bar{C}}_{CO_3}^h \\
&\quad + \int_{\Gamma_d} (\mathbf{B}_{CO_3}^T \cdot \mathbf{t}_{\Gamma_d}) 2h(\xi) \Phi^f k_d(h) (\mathbf{t}_{\Gamma_d}^T \cdot \nabla p_w) \mathbf{N}_{CO_3} d\Gamma \bar{\tilde{C}}_{CO_3}^h \\
&\quad + \int_{\Gamma_d} \mathbf{N}_{CO_3}^T 2h(\xi) \frac{\partial \xi}{\partial t} d\Gamma
\end{aligned} \tag{78}$$

320 References

- 321 [1] M. de Rooij, K. Van Tittelboom, N. De Belie, E. Schlangen, State-of-the-art report of RILEM technical
322 committee 221-SHC: Self-healing phenomena in cement-based materials, Springer Dordrecht Heidel-
323 berg, New York, London, 2013.
- 324 [2] K. Van Tittelboom, N. De Belie, Self-healing in cementitious materials-a review, Materials 6 (6) (2013)
325 2182–2217.
- 326 [3] N. Z. Muhammad, A. Shafaghat, A. Keyvanfar, M. Z. A. Majid, S. Ghoshal, S. E. M. Yasouj, A. A.
327 Ganiyu, M. S. Kouchaksaraei, H. Kamyab, M. M. Taheri, M. R. Shirdar, R. McCaffer, Tests and

- 328 methods of evaluating the self-healing efficiency of concrete: A review, *Construction and Building*
329 *Materials* 112 (2016) 1123–1132.
- 330 [4] C. Edvardsen, Water permeability and autogenous healing of cracks in concrete, *ACI Materials Journal-*
331 *American Concrete Institute* 96 (4) (1999) 448–454.
- 332 [5] A. Neville, Autogenous healing-a concrete miracle ?, *Concrete International* 24 (11).
- 333 [6] F. Ranaivomanana, V. Jérôme, S. Alain, B. Xavier, Sealing process induced by carbonation of localized
334 cracks in cementitious materials, *Cement and Concrete Composites* 37 (2013) 37–46.
- 335 [7] W. De Muynck, N. De Belie, W. Verstraete, Microbial carbonate precipitation in construction materials:
336 a review, *Ecological Engineering* 36 (2) (2010) 118–136.
- 337 [8] V. Wiktor, H. Jonkers, Quantification of crack-healing in novel bacteria-based self-healing concrete,
338 *Cement and Concrete Composites* 33 (7) (2011) 763–770.
- 339 [9] B. Hilloulin, D. Hilloulin, F. Grondin, A. Loukili, N. De Belie, Mechanical regains due to self-healing
340 in cementitious materials: experimental measurements and micro-mechanical model, *CEMENT AND*
341 *CONCRETE RESEARCH* 80 (2016) 21–32.
- 342 [10] A. S. Chitez, A. D. Jefferson, A coupled thermo-hygro-chemical model for characterising autogenous
343 healing in ordinary cementitious materials, *Cement and Concrete Research* 88 (2016) 184–197.
- 344 [11] D. Robert, J. Anthony, Micromechanical modelling of self-healing cementitious materials, *International*
345 *Journal of Solids and Structures* (2017) in press.
- 346 [12] J. J. Remmers, R. de Borst, Numerical modelling of self healing mechanisms, in: *Self Healing Materials*,
347 Springer, 2007, pp. 365–380.
- 348 [13] A. Aliko-Benítez, M. Doblarén, J. Sanz-Herrera, Chemical-diffusive modeling of the self-healing behav-
349 ior in concrete, *International Journal of Solids and Structures* 69-70 (2015) 392–402.
- 350 [14] E. Roubin, A. Vallade, N. Benkemoun, J.-B. Colliat, Multi-scale failure of heterogeneous materials: A
351 double kinematics enhancement for embedded finite element method, *International Journal of Solids*
352 *and Structures* 52 (2015) 180–196.
- 353 [15] N. Benkemoun, M. Hammood, O. Amiri, Embedded finite element formulation for the modeling of
354 chloride diffusion accounting for chloride binding in meso-scale concrete, *Finite Elements in Analysis*
355 *and Design* doi:10.1016/j.finel.2017.03.003.
- 356 [16] J. Simo, M. Rifai, A class of mixed assumed strain methods and the method of incompatible modes.,
357 *International Journal of Numerical Methods in Engineering* 29 (1990) 1595–1638.
- 358 [17] T. Mohammadnejad, A. Khoei, An extended finite element method for hydraulic fracture propagation
359 in deformable porous media with the cohesive crack model, *Finite Elements in Analysis and Design*
360 73 (0) (2013) 77–95.
- 361 [18] J. Réthoré, R. de Borst, M.-A. Abellan, A two-scale approach for fluid flow in fractured porous media,

- 362 International Journal for Numerical Methods in Engineering 71 (7) (2007) 780–800.
- 363 [19] J. Alfaiate, P. Moonen, L. Sluys, J. Carmeliet, On the use of strong discontinuity formulations for the
364 modeling of preferential moisture uptake in fractured porous media, *Computer Methods in Applied
365 Mechanics and Engineering* 199 (45–48) (2010) 2828–2839.
- 366 [20] R. de Borst, A classification of poromechanical interface elements, *Journal of Modeling in Mechanics
367 and Materials*.
- 368 [21] B. Carrier, S. Granet, Numerical modeling of hydraulic fracture problem in permeable medium using
369 cohesive zone model, *Engineering fracture mechanics* 79 (2012) 312–328.
- 370 [22] X. Jourdain, J. Colliat, C. De Sa, F. Benboudjema, F. Gatuingt, Upscaling permeability for fractured
371 concrete: mesomacro numerical approach coupled to strong discontinuities, *International Journal for
372 Numerical and Analytical Methods in Geomechanics* 38 (5) (2013) 536–550.
- 373 [23] N. Benkemoun, R. Gelet, E. Roubin, J.-B. Colliat, Poroelastic two-phase material modeling: theoretical
374 formulation and embedded finite element method implementation, *International Journal for Numerical
375 and Analytical Methods in Geomechanics* 39 (12) (2015) 1255–1275.
- 376 [24] N. Moës, M. Cloirec, P. Cartraud, J.-F. Remacle, A computational approach to handle complex mi-
377 crostructure geometries, *Computer Methods in Applied Mechanics and Engineering* 192 (2003) 3163–
378 3177.
- 379 [25] N. Benkemoun, M. Hammood, O. Amiri, A meso-macro numerical approach for crack-induced diffu-
380 sivity evolution in concrete, *Construction and Building Materials* 10.1016/j.conbuildmat.2017.02.146.
- 381 [26] A. Djerbi, S. Bonnet, A. Khelidj, Influence of traversing crack on chloride diffusion into concrete,
382 *Cement and Concrete Research* 38 (6) (2008) 877–883.